Accepted Manuscript

An exact solution for the 3D MHD stagnation-point flow of a micropolar fluid

A. Borrelli, G. Giantesio, M.C. Patria

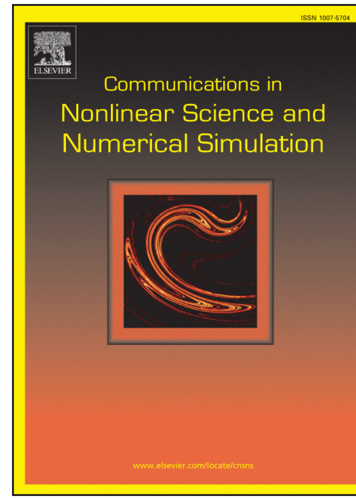

PII: S1007-5704(14)00173-7
DOI: http://dx.doi.org/10.1016/j.cnsns.2014.04.011
Reference: CNSNS 3167

To appear in: *Communications in Nonlinear Science and Numerical Simulation*

Received Date: 17 July 2013
Revised Date: 11 April 2014
Accepted Date: 15 April 2014

Please cite this article as: Borrelli, A., Giantesio, G., Patria, M.C., An exact solution for the 3D MHD stagnation-point flow of a micropolar fluid, *Communications in Nonlinear Science and Numerical Simulation* (2014), doi: http://dx.doi.org/10.1016/j.cnsns.2014.04.011

An exact solution for the 3D MHD stagnation-point flow of a micropolar fluid

A. Borrelli[1], G. Giantesio[1], M.C. Patria[1]

[a]Dipartimento di Matematica e Informatica, Università di Ferrara, via Machiavelli 35, 44121 Ferrara Italy

Abstract

The influence of a non-uniform external magnetic field on the steady three dimensional stagnation-point flow of a micropolar fluid over a rigid uncharged dielectric at rest is studied. The total magnetic field is parallel to the velocity at infinity. It is proved that this flow is possible only in the axisymmetric case. The governing nonlinear partial differential equations are reduced to a system of ordinary differential equations by a similarity transformation, before being solved numerically. The effects of the governing parameters on the fluid flow and on the magnetic field are illustrated graphically and discussed.

Keywords: Micropolar fluids, MHD flow, three-dimensional stagnation-point flow, numerical solutions.
2010 MSC: 76W05, 76D10.

1. Introduction

The recent industrial processes are characterized by the use of new materials which cannot be described by Newtonian fluids. Due to this reason, many non-Newtonian models have been proposed. Among these models, the micropolar fluids have been introduced by Eringen [1] in order to take into consideration the effects of local structure and micro-motions of the fluid particles which cannot be described by the classical models. The incompressible micropolar fluids represent liquids consisting of rigid, randomly oriented spherical particles suspended in a viscous medium, where the deformation of fluid particles is ignored. The related mathematical model is based on the introduction of a new vector field (the microrotation) which describes the total angular velocity of the particles rotation. Hence a new equation is added representing the principle of conservation of local angular momentum. Micropolar fluids describe the behavior of polymeric fluids, exotic lubricants, biological liquids, microemulsions, alloys, colloidal suspensions, polymeric blends and liquid crystals so that they have many applications in the chemical, pharmaceutical, engineering and food industries. In parallel with practical applications ([2], [3], [4]), the theoretical aspects of the solution have been investigated by many authors ([5], [6], [7], [8], [9], [10]).

A very vast amount of research on the effects of an electromagnetic field on the micropolar fluid flow under different conditions and in the presence of various physical effects has been reported ([11], [12], [13], [14], [15], [16], [17], [18], [9], [19]). These efforts have been made to study the MHD problems by many physicists and mathematicians due to their relevant applications, complexity and mathematical challenges. In particular, a relevant physical situation studied by several authors ([20], [21], [22] and the references quoted herein) is when the flow and the magnetic field are aligned at infinity.

An important example of the mutual interaction between the fluid flow and the electromagnetic field is the MHD stagnation-point flow. The orthogonal two-dimensional stagnation-point flow of a Newtonian fluid on a flat plate first studied by Hiemenz ([23]) was extended to the three-dimensional case by Homman ([24]). From the mathematical point of view, stagnation-point flow is an important exact solution of the Navier-Stokes equations which belongs to the similarity solutions class. By similarity transformations, the

Email addresses: brs@unife.it (A. Borrelli), gntgli@unife.it (G. Giantesio), pat@unife.it (M.C. Patria)

PDEs which govern the motion are reduced to a system of ODEs. Similarity solutions describe fundamental physically relevant problems and are used as test for the accuracy of numerical methods. The stagnation-point flow describes physically a jet of fluid which impinges on a rigid body. The problem of stagnation-point flow was extended in numerous ways to include various physical effects ([25], [26], [27], [28]). In particular, as far as the micropolar fluids are concerned, the plane stagnation-point flow was studied in [29], while the three-dimensional one in [30]. Previously Ahmadi [31] obtained self-similar solutions of the boundary layer equations for micropolar flow imposing a condition on the material parameters which make the equations to contain only one parameter. This approach has been followed by several Authors (see for example [32], [33], [34], [4]). We point out that in our research we have not required any condition so that three material parameters appear in the dimensionless ODEs.

In this paper we study the influence of a non-uniform external magnetic field on the steady three dimensional stagnation-point flow of a micropolar fluid. The only published result about this physical situation can be found in [35] for the Newtonian fluids.

We examine the 3D stagnation-point flow of a micropolar fluid filling the half-space $x_2 \geq 0$ when the total magnetic field $\mathbf{H}$ is parallel to the velocity at infinity. We search $\mathbf{H}$ depending on two sufficiently regular unknown functions. The whole space is permeated by a non-uniform external magnetic field $\mathbf{H}_e$ while the external electric field is absent. The expression of $\mathbf{H}_e$ assures that if we consider the 3D stagnation point flow of an inviscid fluid (see [35]) we have that $\mathbf{H}_e$ coincides with the total magnetic field and it is parallel to the fluid velocity in all the half space $x_2 > 0$. Due to the no-slip condition for the velocity of the micropolar fluid at $x_2 = 0$, this alignment is disrupted near the boundary. However, as it is reasonable from the physical point of view, the viscosity effects occur only in a boundary layer and so we require that the total magnetic field and the fluid velocity are parallel at infinity. It is expected that this request is satisfied if the external magnetic field is sufficiently weak.

The region occupied by the fluid is bordered by the boundary of a solid obstacle which is a rigid uncharged dielectric at rest. We underline that many Authors ignore the details of the electromagnetic field in the solid region but the relevance of the problem to any physical situation may be in doubt if we do not join the solution in the fluid to a suitable solution in the solid. In [35] it is proved that the expression of the electromagnetic field in the solid is formally the same independently of the fluid model over the solid.

In the first section we recall the results obtained in [35] when the fluid over the solid is inviscid. The analysis of the inviscid case is very important because, as it is reasonable from the physical point of view, the viscosity occurs only near the boundary. So we assume that at infinity the flow of the micropolar fluid approaches the flow of an inviscid fluid for which the stagnation-point is shifted from the origin.

The goal of this paper is to prove that such steady 3D MHD stagnation-point flow of a micropolar fluid is possible only if the flow is axisymmetric. The study of this problem leads to a non linear ordinary differential problem which depends on three material parameters describing the micropolar nature (c_1, c_2, c_3) and on two parameters R_m (Reynolds number or magnetic Prandtl number) and β_m (Alfvén number) related to the magnetic nature of the flow. By solving numerically the problem, we find that, as usual in stagnation-point flows, the influence of the viscosity appears only in layer lying the boundary whose thickness depends on R_m and β_m. More precisely, it increases as β_m increases, while it decreases as R_m increases.

Some numerical examples and pictures are given in order to illustrate the effects due to the magnetic field on the behavior of the solution. The numerical results are obtained by using the MATLAB routine `bvp4c`, which is described in [36].

2. Preliminaries

Let us consider the steady three-dimensional MHD flow of a homogeneous, incompressible, electrically conducting micropolar fluid near a stagnation-point filling the half-space $\mathcal{S}$ (see Figure 1), given by

$$\mathcal{S} = \{(x_1, x_2, x_3) \in \mathbb{R}^3 : (x_1, x_3) \in \mathbb{R}^2, x_2 > 0\}. \tag{1}$$

The coordinate axes are chosen in order to have that the stagnation-point coincides with the origin and the canonical base of $\mathbb{R}^3$ is denoted by $(\mathbf{e}_1, \mathbf{e}_2, \mathbf{e}_3)$. $\partial\mathcal{S}$, i.e. the plane $x_2 = 0$, is the boundary of a solid which is a rigid uncharged dielectric at rest occupying

$$\mathcal{S}^- = \{(x_1, x_2, x_3) \in \mathbb{R}^3 : (x_1, x_3) \in \mathbb{R}^2, x_2 < 0\}. \tag{2}$$

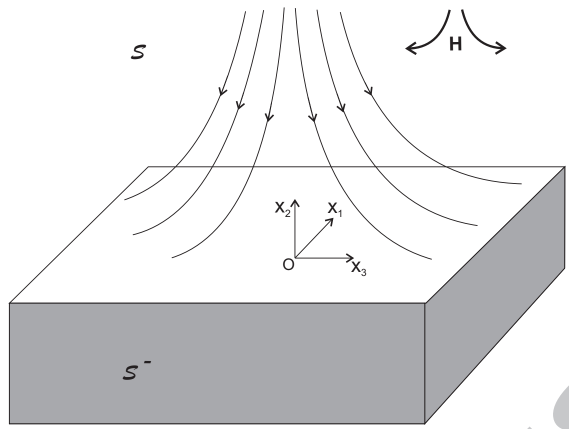

Figure 1: Description flow.

In the absence of free electric charges and external mechanical body forces and body couples, the MHD equations for such a fluid are (see [6])

$$\begin{aligned} &\mathbf{v} \cdot \nabla \mathbf{v} = -\frac{1}{\rho}\nabla p + (\nu + \nu_r)\triangle \mathbf{v} + 2\nu_r(\nabla \times \mathbf{w}) + \frac{\mu_e}{\rho}(\nabla \times \mathbf{H}) \times \mathbf{H}, \\ &\nabla \cdot \mathbf{v} = 0, \\ &I\mathbf{v} \cdot \nabla \mathbf{w} = \lambda \triangle \mathbf{w} + \lambda_0 \nabla(\nabla \cdot \mathbf{w}) - 4\nu_r \mathbf{w} + 2\nu_r(\nabla \times \mathbf{v}), \\ &\nabla \times \mathbf{H} = \sigma_e(\mathbf{E} + \mu_e \mathbf{v} \times \mathbf{H}), \\ &\nabla \times \mathbf{E} = \mathbf{0}, \quad \nabla \cdot \mathbf{E} = 0, \quad \nabla \cdot \mathbf{H} = 0, \qquad \text{in } \mathcal{S}, \end{aligned} \tag{3}$$

where $\mathbf{v}$ is the velocity field, $\mathbf{w}$ is the microrotation field, p is the pressure, $\mathbf{E}$ and $\mathbf{H}$ are the electric and magnetic fields, ρ is the mass density, μ_e is the magnetic permeability, σ_e is the electrical conductivity, ν is the kinematic newtonian viscosity coefficient, ν_r is the microrotation viscosity coefficient, λ, λ_0 are material parameters related to the coefficients of angular viscosity and I is the microinertia coefficient. The previous parameters are positive constants.
We note that in [1] and in [5] equations (3) are slightly different because they are deduced as a special case of a much more general model of microfluids. For the details we refer to [6], p.23.
Moreover we do not employ any condition on the parameters differently from what several Authors do ([31], [33], [34], [4]).

As usual, we impose

$$\mathbf{v}|_{x_2=0} = \mathbf{0}, \quad \mathbf{w}|_{x_2=0} = \mathbf{0} \text{ (strict adherence condition)}, \tag{4}$$

and we ask that the tangential components of $\mathbf{H}$ and $\mathbf{E}$ and the normal components of $\mathbf{B} = \mu_e \mathbf{H}$ and $\mathbf{D} = \epsilon \mathbf{E}$ (ϵ = dielectric constant) are continuous across the plane $x_2 = 0$.

We assume that the external magnetic field

$$\mathbf{H}_e = H_\infty[x_1\mathbf{e}_1 - (c+1)x_2\mathbf{e}_2 + cx_3\mathbf{e}_3], \quad H_\infty = \text{constant}, \quad (x_1, x_2, x_3) \in \mathbb{R}^3, \tag{5}$$

permeates the whole physical space and that the external electric field $\mathbf{E}_e$ is absent. As it is easy to verify, the non degenerate field lines of $\mathbf{H}_e$ belong to the Titeica surfaces $x_1x_2x_3$ =constant which tend to the plane $x_2 = 0$ as $|x_1|, |x_3| \to +\infty$.
We chose the expression (5) for $\mathbf{H}_e$ because if we consider the 3D stagnation point flow of an inviscid fluid (see [35]) we have that it coincides with the total magnetic field and it is parallel to the fluid velocity in all the half space $x_2 > 0$. Due to the no-slip condition for the velocity of the micropolar fluid at $x_2 = 0$, this alignment is disrupted near the boundary. However, as it is reasonable from the physical point of view, the viscosity effects occur only in a boundary layer and so we require that the total magnetic field and the fluid velocity are parallel at infinity. It is expected that this request is satisfied if the external magnetic field is sufficiently weak. The alignment of the velocity and the magnetic field has been studied in several physical situations ([20], [21], [22] and the references quoted herein).

The three-dimensional stagnation-point flow is determined by $\mathbf{v}$, $\mathbf{w}$ in the following form

$$\begin{aligned} &v_1 = ax_1f'(x_2), \quad v_2 = -a[f(x_2) + cg(x_2)], \quad v_3 = acx_3g'(x_2), \\ &w_1 = -cx_3F(x_2), \quad w_2 = 0, \quad w_3 = x_1G(x_2), \qquad (x_1, x_3) \in \mathbb{R}^2, \quad x_2 \in \mathbb{R}^+, \end{aligned} \tag{6}$$

where f, g, F, G are sufficiently regular unknown functions and a, c are some constants. We recall that $(6)_{1,2,3}$ generalize the velocity of an inviscid fluid whose flow is the three dimensional stagnation-point flow pointed to $x_2 = 0$ ([25]). For this reason, we suppose $a > 0$, $c \neq 0$ and we exclude the case $c \leq -1$, because the inviscid fluid moves towards the wall $x_2 = 0$. The dimensionless parameter c is a measure of the three-dimensionality of the motion because the plane orthogonal stagnation-point flow can be obtained by putting $c = 0$.

To satisfy conditions (4) we ask

$$\begin{aligned} &f(0) = 0, \quad f'(0) = 0, \quad g(0) = 0, \quad g'(0) = 0, \\ &F(0) = 0, \quad G(0) = 0. \end{aligned} \tag{7}$$

We seek the total magnetic fields in the fluid and in the solid as

$$\begin{aligned} &\mathbf{H} = H_\infty[x_1h'(x_2)\mathbf{e}_1 - [h(x_2) + ck(x_2)]\mathbf{e}_2 + cx_3k'(x_2)\mathbf{e}_3], \ x_2 \geq 0, \quad \text{and} \\ &\mathbf{H}_s = H_\infty[x_1h_s'(x_2)\mathbf{e}_1 - [h_s(x_2) + ck_s(x_2)]\mathbf{e}_2 + cx_3k_s'(x_2)\mathbf{e}_3], \ x_2 \leq 0, \end{aligned} \tag{8}$$

respectively, where h, k, h_s, k_s are sufficiently regular unknown functions to be determined.

As far as the electromagnetic field in the solid is concerned, in [35] it is proved that if if $\mathbf{H}_s$ is not uniform and its non-degenerate field lines belong to surfaces which asymptote to the plane $x_2 = 0$ as $|x_1|, |x_3| \to +\infty$, then $\mathbf{E}_s = \mathbf{0}$ and

$$\mathbf{H}_s = H_\infty[h'(0)x_1\mathbf{e}_1 - (h'(0) + ck'(0))x_2\mathbf{e}_2 + ck'(0)x_3\mathbf{e}_3], \ x_2 \leq 0, \tag{9}$$

where $h(x_2)$, $k(x_2)$ are the unknown functions in $(8)_1$.

Thanks to the continuity of the normal component of $\mathbf{B}$ across the boundary $x_2 = 0$, from (9) we deduce

$$h(0) + ck(0) = 0, \quad \forall c \in (-1, +\infty), \ c \neq 0,$$

from which follows

$$h(0) = 0, \quad k(0) = 0. \tag{10}$$

As far as the magnetic field in the fluid is concerned, as it is reasonable from the physical point of view, we assume that at infinity the flow of the micropolar fluid approaches the flow of an inviscid fluid whose stagnation-point is shifted from the origin and it is $(0, C, 0)$. Therefore we impose (see [35])

Condition P. *The MHD three-dimensional stagnation-point flow of a micropolar fluid approaches at infinity the flow of an inviscid fluid whose velocity, pressure and magnetic field are given by*

$$\begin{aligned}
&\mathbf{v} = a[x_1\mathbf{e}_1 - (c+1)(x_2 - C)\mathbf{e}_2 + cx_3\mathbf{e}_3],\\
&p = -\frac{1}{2}\rho a^2[x_1^2 + (c+1)^2(x_2 - C)^2 + c^2x_3^2] + p_0,\\
&\mathbf{H} = H_\infty[x_1\mathbf{e}_1 - (c+1)(x_2 - C)\mathbf{e}_2 + cx_3\mathbf{e}_3], \qquad (x_1, x_3) \in \mathbb{R}^2, \quad x_2 \geq C,
\end{aligned} \tag{11}$$

where C and p_0 are constants.

So we append to (3) the following conditions

$$\lim_{x_2\to+\infty} f'(x_2) = 1, \quad \lim_{x_2\to+\infty} g'(x_2) = 1,$$

$$\lim_{x_2\to+\infty} F(x_2) = 0, \quad \lim_{x_2\to+\infty} G(x_2) = 0, \tag{12}$$

$$\lim_{x_2\to+\infty} h'(x_2) = 1, \lim_{x_2\to+\infty} k'(x_2) = 1. \tag{13}$$

The asymptotic behavior of the functions f, g, h and k at infinity depends on the constant C in (11) as

$$\lim_{x_2\to+\infty}[f(x_2) - x_2] = -A, \quad \lim_{x_2\to+\infty}[g(x_2) - x_2] = -B, \tag{14}$$

$$\lim_{x_2\to+\infty}[h(x_2) - x_2] = -A, \quad \lim_{x_2\to+\infty}[k(x_2) - x_2] = -B, \tag{15}$$

$$\begin{aligned}
&\lim_{x_2\to+\infty}[f(x_2) + cg(x_2) - (c+1)x_2] = -(c+1)C,\\
&\lim_{x_2\to+\infty}[h(x_2) + ck(x_2) - (c+1)x_2] = -(c+1)C,
\end{aligned} \tag{16}$$

so that

$$C = \frac{A + cB}{c+1} = \text{displacement thickness.}$$

The constants A, B, C are not assigned a priori, but their values can be found by solving numerically the problem.

We underline that (14) and (15) imply

$$\mathbf{v} \times \mathbf{H} = \mathbf{0} \quad \text{at infinity.} \tag{17}$$

As it is proved in the Appendix, under the no-restrictive hypothesis that

(i) h' vanishes at most at isolated points,

the following theorem holds

Theorem 1. *Let a homogeneous, incompressible, electrically conducting micropolar fluid occupy the half-space $\mathcal{S}$ embedded in the external electromagnetic field $\mathbf{H}_e = H_\infty[x_1\mathbf{e}_1 - (c+1)x_2\mathbf{e}_2 + cx_3\mathbf{e}_3]$, $\mathbf{E}_e = \mathbf{0}$. If the total magnetic field in the solid is (9) and the hypothesis (i) is satisfied, under the assumption $F, G \in L^1([0, +\infty))$, then the steady three-dimensional MHD stagnation-point flow of such a fluid is possible only if the flow is axisymmetric (i.e. $c = 1$, $f = g$, $h = k$, $F = G$ in (6) and $(8)_1$). Moreover $\mathbf{E} = \mathbf{0}$ and*

$$\begin{aligned}
p = &-\rho\frac{a^2}{2}[x_1^2 + 4f^2(x_2) + 4x_3^2] - 2\rho a(\nu + \nu_r)f'(x_2) - 4\nu_r\rho\int_0^{x_2} F(s)ds\\
&-\mu_e\frac{H_\infty^2}{2}(x_1^2 + 4x_3^2)[h'^2(x_2) - 1] + p_0, \qquad (x_1, x_3) \in \mathbb{R}^2, \quad x_2 \in \mathbb{R}^+.
\end{aligned}$$

Therefore

$$\begin{aligned}\mathbf{v} =& a[x_1 f'(x_2)\mathbf{e}_1 - 2f(x_2)\mathbf{e}_2 + x_3 f'(x_2)\mathbf{e}_3], \quad \mathbf{w} = F(x_2)(-x_3\mathbf{e}_1 + x_1\mathbf{e}_3),\\ \mathbf{H} =& H_\infty[x_1 h'(x_2)\mathbf{e}_1 - 2h(x_2)\mathbf{e}_2 + x_3 h'(x_2)\mathbf{e}_3], \quad (x_1, x_3) \in \mathbb{R}^2, \quad x_2 \in \mathbb{R}^+,\end{aligned} \tag{18}$$

with (f, h, F) *solution of the problem*

$$\begin{aligned}&\frac{\nu+\nu_r}{a} f''' + 2ff'' - f'^2 + 1 + 2\frac{\nu_r}{a}F' - \frac{\mu_e}{\rho}\frac{H_\infty^2}{a^2}(2hh'' - h'^2 + 1) = 0,\\ &\lambda F'' + Ia(2F'f - Ff') - 2\nu_r(2F + af'') = 0,\\ &h'' + 2\sigma_e\mu_e a(fh' - hf') = 0,\\ &f(0) = 0,\ f'(0) = 0,\ F(0) = 0,\ h(0) = 0,\\ &\lim_{x_2\to+\infty} f'(x_2) = 1, \ \lim_{x_2\to+\infty} F'(x_2) = 0, \ \lim_{x_2\to+\infty} h'(x_2) = 1.\end{aligned} \tag{19}$$

This theorem also furnishes

$$A = B = C.$$

It is now convenient to rewrite the previous boundary value problem in dimensionless form in order to reduce the number of the material parameters. To this end we put

$$\eta = \frac{x_2}{L}, \quad L = \sqrt{\frac{\nu+\nu_r}{a}}, \quad \varphi(\eta) = \frac{f(L\eta)}{L}, \quad \Phi(\eta) = \frac{2\nu_r}{a^2}\frac{F(L\eta)}{L}, \quad \Psi(\eta) = \frac{h(L\eta)}{L}; \tag{20}$$

so problem (19) becomes

$$\begin{aligned}&\varphi''' + 2\varphi\varphi'' - \varphi'^2 + 1 + \Phi' - \beta_m(2\Psi\Psi'' - \Psi'^2 + 1) = 0,\\ &\Phi'' + 2c_3\Phi'\varphi - \Phi(c_3\varphi' + c_2) - c_1\varphi'' = 0,\\ &\Psi'' + 2R_m(\varphi\Psi' - \Psi\varphi') = 0,\\ &\varphi(0) = 0, \ \varphi'(0) = 0, \ \Phi(0) = 0, \ \Psi(0) = 0,\\ &\lim_{\eta\to+\infty}\varphi'(\eta) = 1, \ \lim_{\eta\to+\infty}\Phi(\eta) = 0, \ \lim_{\eta\to+\infty}\Psi'(\eta) = 1,\end{aligned} \tag{21}$$

where $c_1,\ c_2,\ c_3,\ \beta_m,\ R_m$ are given by

$$\begin{aligned}&c_1 = \frac{4\nu_r^2}{\lambda a}, \quad c_2 = \frac{4\nu_r(\nu+\nu_r)}{\lambda a}, \quad c_3 = \frac{I}{\lambda}(\nu+\nu_r),\\ &\beta_m = \frac{\mu_e}{\rho}\frac{H_\infty^2}{a^2} \text{ (Alfvén number)}, \quad R_m = (\nu+\nu_r)\sigma_e\mu_e \text{ (Reynolds number)}.\end{aligned} \tag{22}$$

We recall that this particular Reynolds number is also known in the literature as the magnetic Prandtl number.

3. Discussion of the flow

As we can see from problem (21), the flow depends on the choice of several parameters: c_1, c_2, c_3 describing the micropolar nature of the fluid, R_m characterizing the electromagnetic and viscosity properties of the fluid and β_m related to the magnetic permeability and to the strength of the external magnetic field. The aim of this Section is to solve numerically problem (21) and to show the influence of the previous parameters on the flow.

The values of R_m and β_m are chosen according to [20]. As far as the value of β_m is concerned, we have that β_m has to be less than 1 in order to preserve the parallelism of $\mathbf{H}$ and $\mathbf{v}$ at infinity, as it will be underlined in the sequel ([35], [20]). The values of c_1, c_2, c_3 are chosen according to [30].

The numerical solution of the problem is computed through the `bvp4c` MATLAB routine. Such a routine is a finite difference code that implements the three-stage Lobatto IIIa formula. This is a collocation formula and here the collocation polynomial provides a C^1-continuous solution that is fourth-order accurate uniformly in $[0, 5]$. Mesh selection and error control are based on the residual of the continuous solution. We set the relative and the absolute tolerance equal to 10^{-7}. The method was used and described in [36].

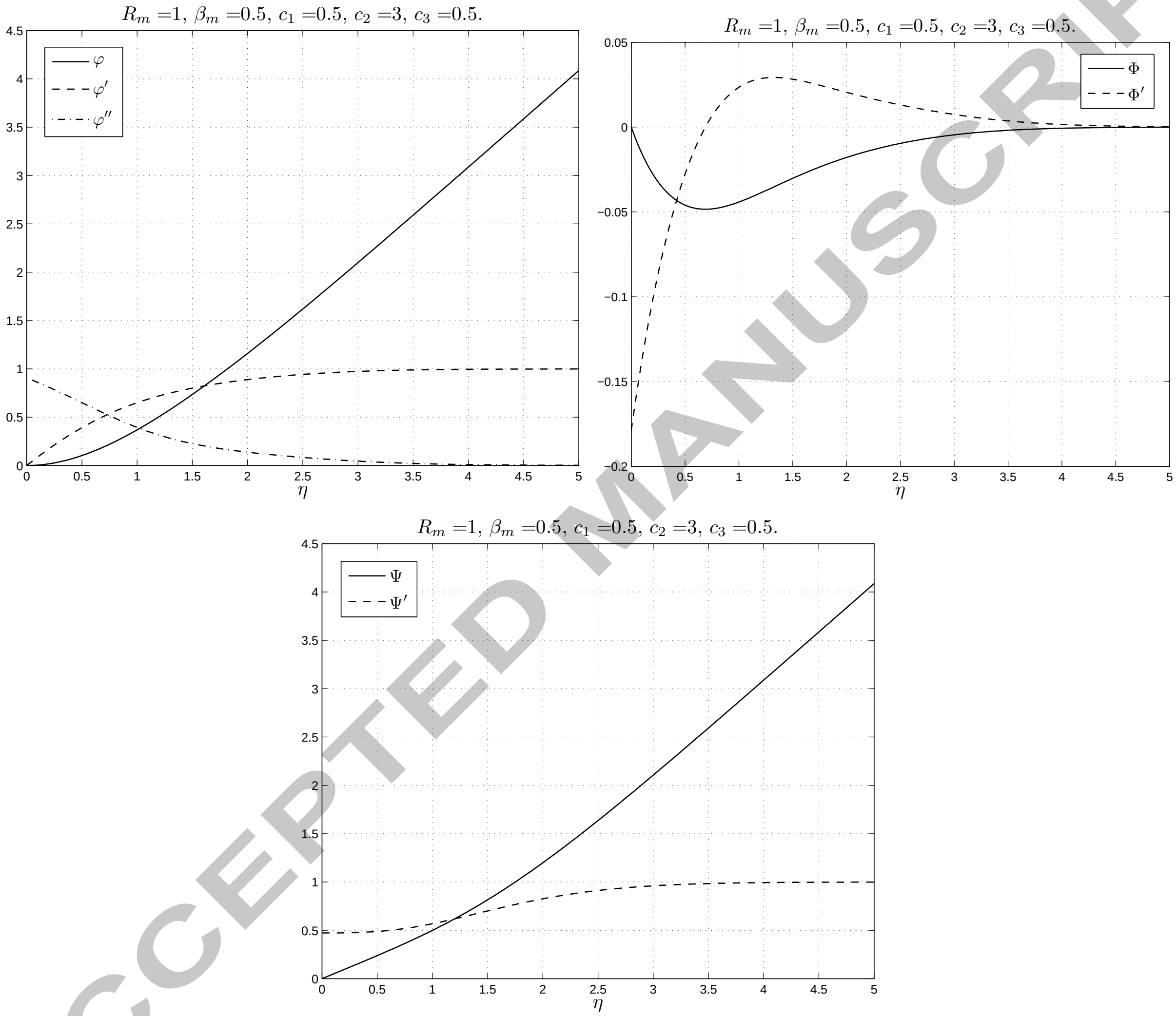

Figure 2: The first figure shows the velocity $(\varphi, \varphi', \varphi'')$, the second the microrotation (Φ, Φ') and the third the total magnetic field (Ψ, Ψ').

In Figure 2_1 we plot the profiles $\varphi, \varphi', \varphi''$ when $c_1 = 0.5$, $c_2 = 3.0$, $c_3 = 0.5$, $R_m = 1$ and $\beta_m = 0.5$, while Figure 2_2 shows the behavior of Φ, Φ' for the same values of the parameters. The trend of Ψ, Ψ' is given in Figure 2_3.
We recall that these functions has a relevant physical meaning:

- φ describes the velocity

$$\mathbf{v} = a[x_1\varphi'(\eta)\mathbf{e}_1 - 2L\varphi(\eta)\mathbf{e}_2 + x_3\varphi'(\eta)\mathbf{e}_3];$$

- Φ characterizes the microrotation

$$\mathbf{w} = \frac{a^2L}{2\nu_r}\Phi(\eta)(-x_3\mathbf{e}_1 + x_1\mathbf{e}_3);$$

- Ψ determines the total magnetic field

$$\mathbf{H} = H_\infty[x_1\Psi'(\eta)\mathbf{e}_1 - 2L\Psi(\eta)\mathbf{e}_2 + x_3\Psi'(\eta)\mathbf{e}_3].$$

Hence Figure 2 represents the behavior of the velocity, the microrotation and the total magnetic field.

We have plotted the profiles of $\varphi,\ \varphi',\ \varphi'',\ \Phi,\ \Phi',\ \Psi,\ \Psi'$ only for these values of the parameters because they have an analogous behavior for $c_1 \neq 0.5$, $c_2 \neq 3.0$, $c_3 \neq 0.5$, $R_m \neq 1$ and $\beta_m \neq 0.5$.

As one can see from Figure 2, the numerical solution $(\varphi,\ \Phi,\ \Psi)$ of problem (21) satisfies

$$\lim_{\eta\to+\infty}[\varphi(\eta) - \eta] = -\alpha, \quad \lim_{\eta\to+\infty}\Phi(\eta) = 0, \quad \lim_{\eta\to+\infty}[\Psi(\eta) - \eta] = -\alpha, \text{ with } \alpha = \frac{A}{L}.$$

The parameter α is proportional to the displacement thickness which represents the quote of the plane towards which the inviscid fluid, whose flow is approached at infnity by the micropolar fluid, is pointed. We denote by

- $\overline{\eta}_\varphi$ the value of η such that if $\eta > \overline{\eta}_\varphi$ then $\varphi \cong \eta - \alpha$;
- $\overline{\eta}_\Phi$ the value of η such that if $\eta > \overline{\eta}_\Phi$, then $\Phi \cong 0$.

The values of $\overline{\eta}_\varphi$ and $\overline{\eta}_\Phi$ are computed numerically by requiring an accuracy of at least 99%.
Thanks to these notations, the influence of the viscosity on the velocity and on the microrotation appears only in a layer lining the boundary whose thickness is $\overline{\eta}_\varphi$ for the velocity and $\overline{\eta}_\Phi$ for the microrotation. The thickness δ of the boundary layer for the flow is defined as

$$\delta := \max(\overline{\eta}_\varphi, \overline{\eta}_\Phi).$$

As it can be expected from the physical point of view, beyond the boundary layer the fluid behaves as an inviscid one.

In order to study the influence of the parameters $c_1,\ c_2,\ c_3,\ \beta_m$ and R_m on the motion we provide Table 1. Actually, this Table shows the values of $\varphi''(0)$, $\Psi'(0)$, $\Phi'(0)$, α, $\overline{\eta}_\varphi$, $\overline{\eta}_\Phi$, δ. These quantities are important from a physical point of view:

- $\varphi''(0)$ and $\Phi'(0)$ furnish the skin friction ($\tau_\mathbf{0}$) and the skin couple friction ($\gamma_\mathbf{0}$) at $x_2 = 0$:

$$\tau_\mathbf{0} = \rho a^2 L\varphi''(0)(x_1\mathbf{e}_1 + x_3\mathbf{e}_3),$$
$$\gamma_\mathbf{0} = -\rho\lambda\frac{a^2}{2\nu_r}\Phi'(0)(x_3\mathbf{e}_1 - x_1\mathbf{e}_3);$$

- $\Psi'(0)$ determines the magnetic field on the boundary of the obstacle:

$$\mathbf{H}|_{\eta=0} = H_\infty\Psi'(0)(x_1\mathbf{e}_1 + x_3\mathbf{e}_3); \tag{23}$$

- α is proportional to the displacement thickness C;
- $\overline{\eta}_\varphi$, $\overline{\eta}_\Phi$, δ are related to the thickness of the boundary layer.

Table 1: Descriptive quantities of the motion for several values of c_1, c_2, c_3, R_m and β_m.

R_m	β_m	c_1	c_2	c_3	$\varphi''(0)$	$\Psi'(0)$	$\Phi'(0)$	α	$\overline{\eta}_\varphi$	$\overline{\eta}_\Phi$	δ
1	0.20	0.10	1.50	0.10	1.1706	0.5311	-0.0523	0.6646	2.4608	1.5755	2.4608
				0.50	1.1723	0.5313	-0.0497	0.6648	2.4775	1.2271	2.4775
			3.00	0.10	1.1737	0.5313	-0.0436	0.6652	2.4775	0.9920	2.4775
				0.50	1.1745	0.5314	-0.0425	0.6653	2.4858	0.7886	2.4858
		0.50	1.50	0.10	1.1275	0.5311	-0.2615	0.6527	2.2941	2.8560	2.8560
				0.50	1.1364	0.5321	-0.2491	0.6536	2.3691	2.2341	2.3691
			3.00	0.10	1.1436	0.5319	-0.2181	0.6560	2.3791	2.3391	2.3791
				0.50	1.1474	0.5323	-0.2127	0.6564	2.4141	2.0090	2.4141
	0.50	0.10	1.50	0.10	0.9267	0.4717	-0.0447	0.9255	3.5362	1.8356	3.5362
				0.50	0.9284	0.4720	-0.0427	0.9256	3.5545	1.3821	3.5545
			3.00	0.10	0.9301	0.4719	-0.0365	0.9265	3.5545	0.8903	3.5545
				0.50	0.9308	0.4720	-0.0357	0.9266	3.5612	0.6852	3.5612
		0.50	1.50	0.10	0.8845	0.4712	-0.2234	0.9084	3.3628	3.4478	3.4478
				0.50	0.8934	0.4726	-0.2138	0.9089	3.4578	2.7376	3.4578
			3.00	0.10	0.9020	0.4723	-0.1825	0.9134	3.4595	2.8826	3.4595
				0.50	0.9056	0.4729	-0.1787	0.9136	3.4962	2.4658	3.4962
100	0.20	0.10	1.50	0.10	1.1604	0.1608	-0.0528	0.6346	2.1290	1.5672	2.1290
				0.50	1.1621	0.1609	-0.0502	0.6348	2.1424	1.2371	2.1424
			3.00	0.10	1.1635	0.1610	-0.0440	0.6353	2.1474	1.0353	2.1474
				0.50	1.1643	0.1611	-0.0429	0.6354	2.1541	0.8419	2.1541
		0.50	1.50	0.10	1.1170	0.1587	-0.2645	0.6219	1.9607	2.7409	2.7409
				0.50	1.1260	0.1594	-0.2515	0.6231	2.0123	2.1507	2.1507
			3.00	0.10	1.1330	0.1597	-0.2202	0.6255	2.0340	2.2491	2.2491
				0.50	1.1370	0.1601	-0.2146	0.6261	2.0640	1.9440	2.0640
	0.50	0.10	1.50	0.10	0.9114	0.1386	-0.0465	0.8048	2.6942	1.8123	2.6942
				0.50	0.9133	0.1388	-0.0442	0.8052	2.7192	1.4205	2.7192
			3.00	0.10	0.9149	0.1389	-0.0378	0.8061	2.7226	1.1320	2.7226
				0.50	0.9156	0.1389	-0.0369	0.8063	2.7326	0.8853	2.7326
		0.50	1.50	0.10	0.8683	0.1363	-0.2329	0.7835	2.4441	3.0610	3.0610
				0.50	0.8778	0.1371	-0.2218	0.7856	2.5442	2.4375	2.5442
			3.00	0.10	0.8858	0.1375	-0.1892	0.7904	2.5675	2.5642	2.5675
				0.50	0.8898	0.1379	-0.1848	0.7914	2.6175	2.2241	2.6175

From Table 1 we can make some considerations on the influence of the parameters on these quantities. First of all, we see that if we fix two parameters among c_1, c_2, c_3, then the values of α, $\varphi''(0)$, $\Phi'(0)$

- increase as c_2 or c_3 increases;
- decrease as c_1 increases.

Figures from 3 to 5 elucidate the dependence of the functions φ', Φ on the parameters c_1, c_2, c_3. We can see that the function which appears most influenced by c_1, c_2, c_3 is Φ, in other words the microrotation. More precisely, the profile of Φ rises as c_2 or c_3 increases and c_1 decreases; c_1 is the parameter that most influences the microrotation. The other function, φ', does not show considerable variations as c_1, c_2, c_3 assume different values. This behavior is the same as in the absence of the electromagnetic field or when the electromagnetic field is uniform ([30], [13]).

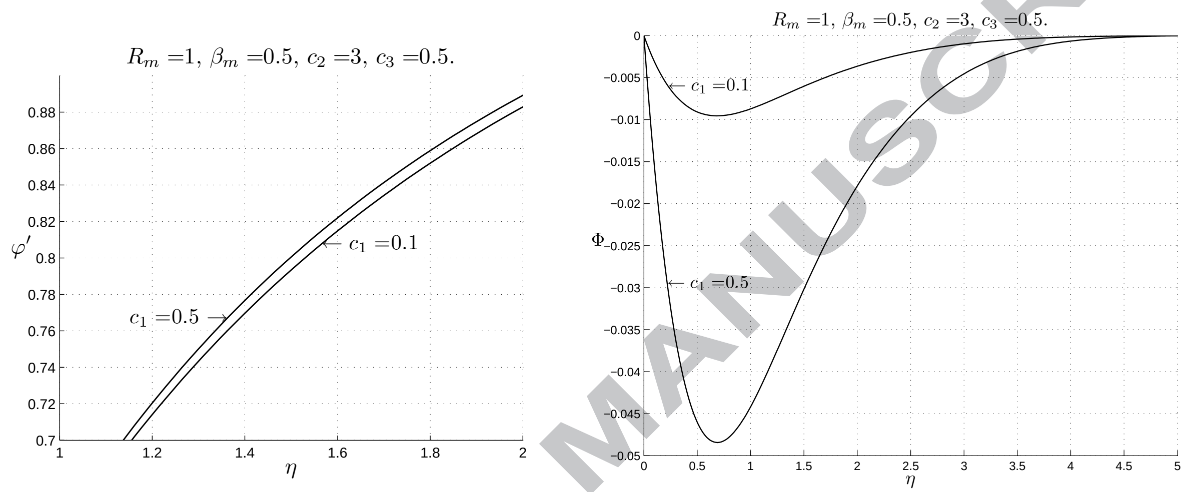

Figure 3: φ', Φ profiles when c_1 changes.

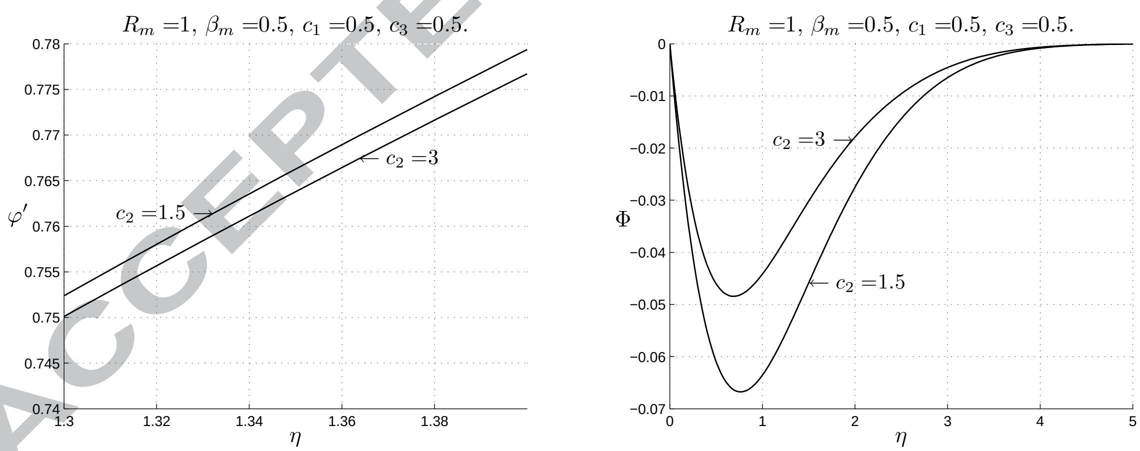

Figure 4: φ', Φ profiles when c_2 changes.

As far as the dependence on R_m and β_m is concerned, from Table 1 we have that:

- if β_m increases, then α and $\Phi'(0)$ increase, while $\varphi''(0)$ and $\Psi'(0)$ decrease;

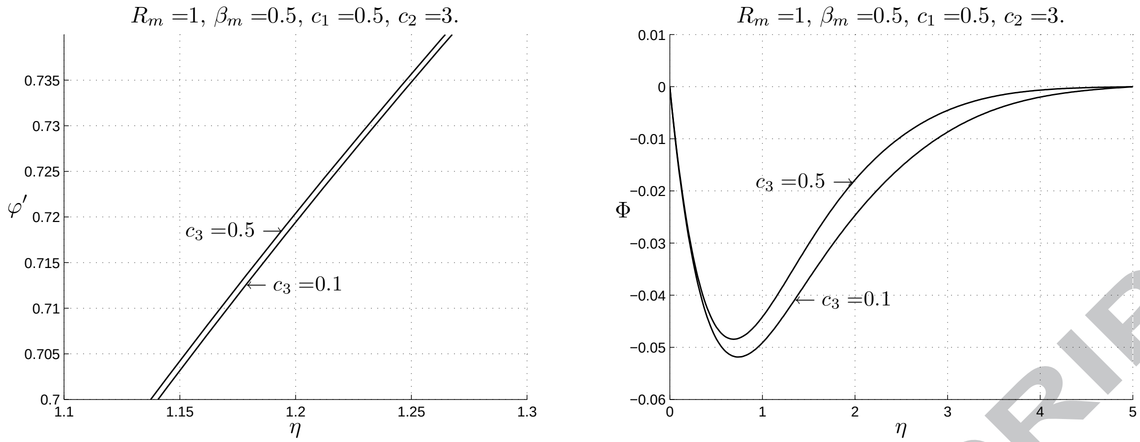

Figure 5: φ', Φ profiles when c_3 changes.

- if R_m increases, then α, $\varphi''(0)$, $|\Phi'(0)|$ and $\Psi'(0)$ decrease.

Table 1 underlines that the thickness of the boundary layer depends on R_m and β_m. As in the Newtonian case ([35]), it increases when β_m increases (as is easy to see in Figures 6_1 and 6_2), while it decreases when R_m increases (as is easy to see in Figures 6_3 and 6_4). This behavior is not surprising because β_m is a measure of the strength of the applied magnetic field and as it is underlined in [20] when the magnetic field is strong the disturbances are no longer contained within a boundary layer along the wall. This means that boundary conditions can no longer be prescribed at infinity. In particular, in [20] it is proved that in a perfectly conducting fluid the displacement thickness becomes infinite as β_m goes to 1^-.

To compare the thickness of the boundary layer in different physical situations, we provide Table 2.

Table 2: Boundary layer in the plane orthogonal (δ_{orth}) and in the three-dimensional (δ) stagnation-point flow.

R_m	β_m	c_1	c_2	c_3	δ_{orth}	δ
1	0.20	0.10	1.50	0.10	3.0960	2.4608
		0.50	3.00	0.50	3.0310	2.4141
	0.50	0.10	1.50	0.10	4.2831	3.5362
		0.50	3.00	0.50	4.2431	3.4962
100	0.20	0.10	1.50	0.10	2.5992	2.1290
		0.50	3.00	0.50	2.5042	2.0640
	0.50	0.10	1.50	0.10	3.2894	2.6942
		0.50	3.00	0.50	3.1761	2.6175

More precisely, in Table 2 we have listed the values of the thickness of the boundary layer in the plane orthogonal ([14]) and three dimensional flow when the magnetic field is aligned to the velocity at infinity. As one can see, in the present case (3D) δ is slightly smaller than δ_{orth}. We recall that in the absence of the electromagnetic field ([13]), δ is 1.9071 ($c = 1$, $c_1 = c_3 = 0.1$, $c_2 = 1.5$) and 1.8464 ($c = 1$, $c_1 = c_3 = 0.5$, $c_2 = 3.0$). These numerical results show that the magnetic field $(18)_3$ increases the thickness of the boundary layer.
In [13] it is also been studied the influence of a uniform magnetic field on the 3D flow and it has been underlined that the strength of the magnetic field reduces δ, differently from the present study.

Moreover, as in [13], it is possible to classify the stagnation-point as nodal or saddle point and as attachment or separation point. Since $\varphi''(0)$ is positive, the origin is always a nodal point of attachment.

Finally, we notice that the micropolar nature of the fluid reduces all the descriptive quantities of the motion in comparison to those of the Newtonian fluid, especially the thickness of the boundary layer for the

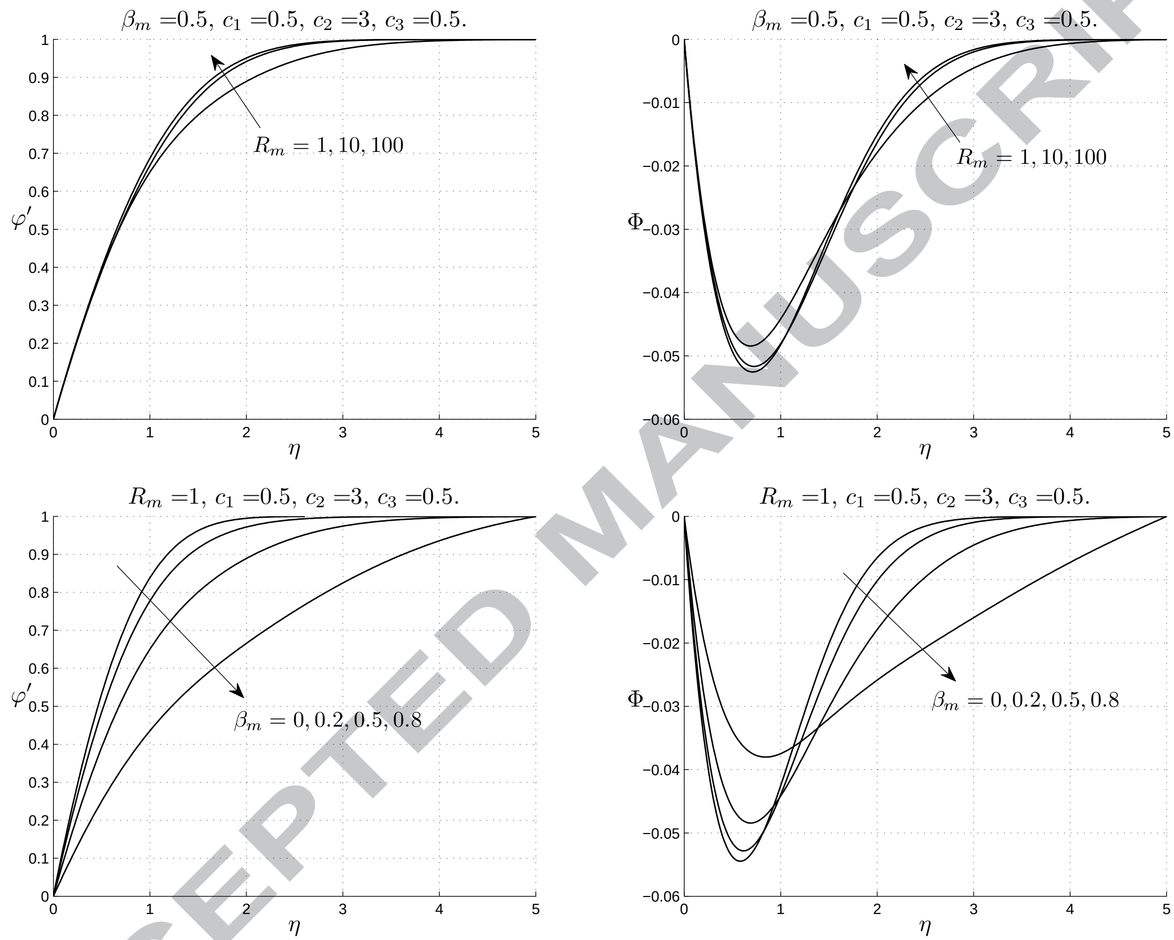

Figure 6: Plots showing the thickness of the boundary layer for different R_m and β_m, respectively.

velocity ([35]).

4. Conclusions

In this paper we study the MHD three-dimensional stagnation-point flow of a micropolar fluid when the total magnetic field is aligned to the velocity at infinity. The region where the fluid motion occurs is bordered by the boundary of a solid obstacle which is a rigid uncharged dielectric at rest. By means of similarity transformations, we reduce the MHD PDEs to a nonlinear system of ODEs which depends on three material parameters c_1, c_2, c_3 describing the micropolar nature of the flow and on two parameters R_m (Reynolds or magnetic Prandtl number) and β_m (Alfvén number) related to the magnetic effects. This system has been numerically integrated.
The results obtained show that

- The total magnetic field is parallel to the velocity at infinity only if the flow is axisymmetric.
- The thickness of the layer where the viscosity effects appear (boundary layer) depends in a relevant way on R_m and β_m and it is smaller than that in the Newtonian case ([35]).
- The alignment of the magnetic field and of the velocity increases the thickness of the boundary layer in comparison to the case in the absence of the magnetic field and when a uniform magnetic field is applied ([13]).
- The displacement thickness increases as c_2, c_3, β_m increase and c_1, R_m decrease.
- The total magnetic field on the boundary of the solid obstacle increases as β_m, R_m decrease and it is not influenced by the micropolar parameter c_1, c_2, c_3.
- The skin friction increases as c_2, c_3 increase and c_1, β_m, R_m decrease.
- The strength of the skin couple friction increases as c_1 increase and c_2, c_3, β_m, R_m decrease.
- Among the three micropolar parameters c_1, c_2, c_3, the parameter c_1 is the one which influences most the motion.
- The micropolar nature of the fluid reduces all the descriptive quantities of the flow in comparison to the Newtonian case.

Acknoledgement
This work was performed under the auspices of G.N.F.M. of INdAM and supported by Italian MIUR.
The authors are grateful to the reviewers for the useful and valuable suggestions which have improved the quality of the work.

5. Appendix

Proof of Theorem 1:
Let $\mathbf{E} = E_1\mathbf{e}_1 + E_2\mathbf{e}_2 + E_3\mathbf{e}_3$ be the total electric field. Then the transmission conditions across the boundary and the fact that $\mathcal{S}^-$ is occupied by a rigid uncharged dielectric at rest require that

$$E_1 = 0,\ E_3 = 0 \ \text{ at } \ x_2 = 0. \tag{24}$$

From $(3)_5$ follows that

$$\mathbf{E} = -\nabla\psi, \ \text{(with } \psi \in C^2(\mathcal{S}) \text{ electrostatic potential)},$$

and equation $(3)_4$ furnishes

$$\begin{aligned}
\frac{\partial\psi}{\partial x_1} &= -\frac{H_\infty}{\sigma_e} c x_3 \{k''(x_2) + \sigma_e\mu_e a[(f(x_2)+cg(x_2))k'(x_2) - (h(x_2)+ck(x_2))g'(x_2)]\},\\
\frac{\partial\psi}{\partial x_2} &= H_\infty \mu_e a c x_1 x_3 [h'(x_2)g'(x_2) - k'(x_2)f'(x_2)],\\
\frac{\partial\psi}{\partial x_3} &= -\frac{H_\infty}{\sigma_e} x_1 \{-h''(x_2) - \sigma_e\mu_e a[(f(x_2)+cg(x_2))h'(x_2) - (h(x_2)+ck(x_2))f'(x_2)]\}.
\end{aligned} \tag{25}$$

Since $\mathbf{E}$ is divergence free, from $(25)_2$, we get

$$[h'(x_2)g'(x_2) - k'(x_2)f'(x_2)]' = 0, \quad x_2 \in \mathbb{R}^+,$$

which due to the conditions at infinity $(12)_{1,2}$ and (13), gives

$$h'(x_2)g'(x_2) = k'(x_2)f'(x_2), \quad \forall x_2 \in \mathbb{R}^+. \tag{26}$$

The previous equality implies the following relationships of proportionality

$$k'(x_2) = l(x_2)h'(x_2), \quad g'(x_2) = l(x_2)f'(x_2), \tag{27}$$

where $l = l(x_2)$ is a sufficiently regular unknown function satisfying the condition

$$\lim_{x_2\to+\infty} l(x_2) = 1. \tag{28}$$

From (26) we have $\psi = \psi(x_1, x_3)$. Then from $(25)_{1,3}$ and from the behavior at infinity ($(12)_{1,2}$, (13), (14), (15)) we deduce

$$\begin{aligned}
&k''(x_2) + \sigma_e\mu_e a[(f(x_2)+cg(x_2))k'(x_2) - (h(x_2)+ck(x_2))g'(x_2)] = 0,\\
&h''(x_2) + \sigma_e\mu_e a[(f(x_2)+cg(x_2))h'(x_2) - (h(x_2)+ck(x_2))f'(x_2)] = 0.
\end{aligned} \tag{29}$$

Hence

$$\mathbf{E} = \mathbf{0}.$$

If we substitute (27) into $(29)_1$, then we obtain

$$lh'' + l'h' + \sigma_e\mu_e a[(f+cg)lh' - (h+ck)lf'] = 0, \tag{30}$$

which by virtue of $(29)_2$ reduces to

$$l'(x_2)h'(x_2) = 0, \quad \forall x_2 \in \mathbb{R}^+. \tag{31}$$

From relation (31), hypothesis (i) and (28), we find

$$l(x_2) \equiv 1, \quad \forall x_2 \in \mathbb{R}^+,$$

so that the relationships (27) are reduced to

$$k'(x_2) = h'(x_2), \quad g'(x_2) = f'(x_2). \tag{32}$$

Thanks to (10) and (32), we have

$$k(x_2) = h(x_2), \quad g(x_2) = f(x_2), \quad \forall x_2 \in \mathbb{R}^+, \quad \text{and} \quad A = B = C. \tag{33}$$

On substituting (32) into (29), we find that h has to satisfy

$$h''(x_2) + \sigma_e\mu_e a(c+1)[f(x_2)h'(x_2) - h(x_2)f'(x_2)] = 0. \tag{34}$$

In order to determine $p,\ f,\ F,\ G$, we substitute (33), and (6) into $(3)_{1,3}$ so that we have

$$
\begin{aligned}
&ax_1\left[(\nu+\nu_r)f''' + a(c+1)ff'' - af'^2 + \frac{2\nu_r}{a}G' - \frac{\mu_e}{\rho a}H^2_\infty(c+1)hh''\right] = \frac{1}{\rho}\frac{\partial p}{\partial x_1},\\
&(\nu+\nu_r)a(c+1)f'' + a^2(c+1)^2 ff' + 2\nu_r(cF+G) + \frac{\mu_e}{\rho}H^2_\infty[x_1^2 + c^2x_3^2]h'h'' = -\frac{1}{\rho}\frac{\partial p}{\partial x_2},\\
&acx_3\left[(\nu+\nu_r)f''' + a(c+1)ff'' - acf'^2 + \frac{2\nu_r}{a}F' - \frac{\mu_e}{\rho a}H^2_\infty(c+1)hh''\right] = \frac{1}{\rho}\frac{\partial p}{\partial x_3},\\
&\lambda F'' + Ia[F'(f+cg) - cFg'] - 2\nu_r(2F + ag'') = 0,\\
&\lambda G'' + Ia[G'(f+cg) - Gf'] - 2\nu_r(2G + af'') = 0.
\end{aligned} \tag{35}
$$

By integrating $(35)_2$ and supposing that, far from the wall, the pressure p has the same behavior as for an inviscid fluid, whose pressure is given by $(11)_2$, we find

$$
\begin{aligned}
p = &-\rho\frac{a^2}{2}[x_1^2 + (c+1)^2 f^2(x_2) + c^2x_3^2] - \rho a(\nu+\nu_r)(c+1)f'(x_2)\\
&-2\nu_r\rho\int_0^{x_2}[cF(s)+G(s)]ds - \mu_e\frac{H^2_\infty}{2}(x_1^2 + c^2x_3^2)[h'^2(x_2) - 1] + p_0.
\end{aligned} \tag{36}
$$

So by $(35)_{1,3}$, we obtain

$$
\begin{aligned}
&\frac{\nu+\nu_r}{a}f''' + (c+1)ff'' - f'^2 + 1 + \frac{2\nu_r}{a^2}G' - \frac{\mu_e}{\rho}\frac{H^2_\infty}{a^2}[(c+1)hh'' - h'^2 + 1] = 0,\\
&\frac{\nu+\nu_r}{a}f''' + (c+1)ff'' - cf'^2 + c + \frac{2\nu_r}{a^2}F' - \frac{\mu_e}{\rho}\frac{H^2_\infty}{a^2}[(c+1)hh'' - ch'^2 + c] = 0.
\end{aligned} \tag{37}
$$

If we use the transformations (20) and we put $\Gamma(\eta) = \dfrac{2\nu_r}{a^2}\dfrac{G(L\eta)}{L}$, then (37), $(35)_{4,5}$, (34) can be written in dimensionless form as

$$
\begin{aligned}
&\varphi''' + (c+1)\varphi\varphi'' - \varphi'^2 + 1 + \Gamma' - \beta_m[(c+1)\Psi\Psi'' - \Psi'^2 + 1] = 0,\\
&\varphi''' + (c+1)\varphi\varphi'' - c\varphi'^2 + c + \Phi' - \beta_m[(c+1)\Psi\Psi'' - c\Psi'^2 + c] = 0,\\
&\Phi'' + c_3(c+1)\Phi'\varphi - \Phi(cc_3\varphi' + c_2) - c_1\varphi'' = 0,\\
&\Gamma'' + c_3(c+1)\Gamma'\varphi - \Gamma(c_3\varphi' + c_2) - c_1\varphi'' = 0,\\
&\Psi'' + R_m(c+1)(\varphi\Psi' - \Psi\varphi') = 0,
\end{aligned} \tag{38}
$$

where $c_1,\ c_2,\ c_3,\ \beta_m,\ R_m$ are given by (22).

The boundary conditions (7), (12), (13) and (10) in dimensionless form become:

$$
\begin{aligned}
&\varphi(0) = 0,\quad \varphi'(0) = 0,\quad \Phi(0) = 0,\quad \Gamma(0) = 0,\quad \Psi(0) = 0,\\
&\lim_{\eta\to+\infty}\varphi'(\eta) = 1,\quad \lim_{\eta\to+\infty}\Phi(\eta) = 0,\quad \lim_{\eta\to+\infty}\Gamma(\eta) = 0,\quad \lim_{\eta\to+\infty}\Psi'(\eta) = 1.
\end{aligned} \tag{39}
$$

We note that the equations $(38)_{1,2}$ are compatible if, and only if,

$$
(c-1)[\varphi'^2 - 1 - \beta_m(\Psi'^2 - 1)] + \Gamma' - \Phi' = 0. \tag{40}
$$

We now show that $c = 1$.
By contradiction, suppose $c \neq 1$.

Computing (40), (38) at $\eta = 0$ gives

$$\begin{aligned}
&\Phi'(0) - \Gamma'(0) = (c-1)[-\beta_m \Psi'^2(0) + \beta_m - 1],\\
&\Gamma'(0) = \beta_m[1 - \Psi'^2(0)] - \varphi'''(0) - 1,\\
&\Phi'(0) = c\beta_m[1 - \Psi'^2(0)] - \varphi'''(0) - c,\\
&\Phi''(0) = c_1\varphi''(0) = \Gamma''(0), \quad \Psi''(0) = 0.
\end{aligned} \tag{41}$$

If we differentiate $(38)_{3,4}$, then it follows

$$\begin{aligned}
&\Gamma'''(0) = -c_2[\beta_m \Psi'^2(0) + 1 - \beta_m] + (c_1 - c_2)\varphi'''(0),\\
&\Phi'''(0) - \Gamma'''(0) = -c_2(c-1)[\beta_m \Psi'^2(0) + 1 - \beta_m],
\end{aligned} \tag{42}$$

where we have used $(41)_{1,2}$.

Differentiating $(38)_5$ and (40) furnishes

$$\Psi'''(0) = 0, \ \Phi'''(0) - \Gamma'''(0) = 2(c-1)\varphi''^2(0). \tag{43}$$

By equating $(42)_2$ and $(43)_2$, since $c \neq 1$ we get

$$\Psi'^2(0) = \frac{1}{\beta_m}\left[-\frac{2}{c_2}\varphi''^2(0) + \beta_m - 1\right], \tag{44}$$

which gives the absurdum if $\beta_m < 1$.

We now turn to the case $\beta_m \geq 1$.
On substituting (44) into $(41)_{2,3}$, we obtain

$$\Gamma'(0) = \frac{2}{c_2}\varphi''^2(0) - \varphi'''(0), \quad \Phi'(0) = \frac{2c}{c_2}\varphi''^2(0) - \varphi'''(0). \tag{45}$$

The twice differentiation of $(38)_{3,4}$ together with (45) and $(41)_4$ gives

$$\Phi^{IV}(0) - \Gamma^{IV}(0) = 2c_3(c-1)\varphi''(0)\left[\frac{(c+1)}{c_2}\varphi''^2(0) - \varphi'''(0)\right]. \tag{46}$$

Evaluating in $\eta = 0$ the twice differentiation of $(38)_5$ and (40) furnishes

$$\begin{aligned}
&\Psi^{IV}(0) = R_m(c+1)\Psi'(0)\varphi''(0),\\
&\Phi^{IV}(0) - \Gamma^{IV}(0) = 2(c-1)\varphi''(0)\left[3\varphi'''(0) + R_m(c+1)\left(\frac{2}{c_2}\varphi''^2(0) + 1 - \beta_m\right)\right].
\end{aligned} \tag{47}$$

If we equate (46) and $(47)_2$, taking into account that $c \neq 1$, we arrive at

$$\left[(3 + c_3)\varphi'''(0) + \frac{(c+1)}{c_2}(2R_m - c_3)\varphi''^2(0) + R_m(c+1)(1 - \beta_m)\right]\varphi''(0) = 0. \tag{48}$$

From the last equation, the proof falls naturally into two cases

(A) $\varphi''(0) \neq 0$ and

$$\varphi'''(0) = -\frac{c+1}{3+c_3}\left[\frac{2R_m - c_3}{c_2}\varphi''^2(0) + R_m(1 - \beta_m)\right]; \tag{49}$$

(B) $\varphi''(0) = 0$.

We first consider case (A).
Differentiating three times of $(38)_3$ gives

$$\Phi^V(0) - \Gamma^V(0) = (c-1)\Big\{(3c_3c_1 + 2c_2)\varphi''^2(0) + c_3\Big[\frac{4}{c_2}(c+1)\varphi''^2(0) - 3\varphi'''(0)\Big]\varphi'''(0)\Big\}, \tag{50}$$

where we used $(43)_2$, $(41)_4$, (45).
If we differentiate $(38)_1$ and we use $(41)_{4,5}$, than we have

$$\varphi^{IV}(0) = -c_1\varphi''(0). \tag{51}$$

Thanks to (44) and (51), from another differentiation of $(38)_5$ and (40), we get

$$\begin{aligned}
\Psi^V(0) &= 2R_m(c+1)[\Psi'(0)\varphi'''(0)],\\
\Phi^V(0) - \Gamma^V(0) &= 2(c-1)\Big\{3\varphi'''^2(0) + 2R_m(c+1)\Big[\frac{2}{c_2}\varphi''^2(0) + 1 - \beta_m\Big]\varphi'''(0) - 4c_1\varphi''^2(0)\Big\}.
\end{aligned} \tag{52}$$

Matching (50) and $(52)_2$, since $c \neq 1$, it holds

$$3(2+c_3)\varphi'''^2(0) + 4(c+1)\left[\frac{2R_m - c_3}{c_2}\varphi''^2(0) + R_m(1-\beta_m)\right]\varphi'''(0) - (8c_1 + 3c_1c_3 + 2c_2)\varphi''^2(0) = 0. \tag{53}$$

Substituting (49) into (53), we get the absurdum

$$\varphi'''^2(0) = -\frac{8c_1 + 3c_1c_3 + 2c_2}{6 + c_3}\varphi''^2(0), \tag{54}$$

because $c_1,\ c_2,\ c_3$ are positive constants and $\varphi''(0) \neq 0$ by assumption.

We now proceed with case (B).
The hypothesis $\varphi''(0) = 0$ simplifies the previous relationships in the following way

$$\begin{aligned}
&\varphi^{IV}(0) = 0, \quad \Psi'^2(0) = \frac{\beta_m - 1}{\beta_m}, \quad \Psi^{IV}(0) = 0,\\
&\Phi'(0) = \Gamma'(0) = -\varphi'''(0), \quad \Phi''(0) = \Gamma''(0) = 0,\\
&\Phi'''(0) = \Gamma'''(0) = (c_1 - c_2)\varphi'''(0), \quad \Phi^{IV}(0) = \Gamma^{IV}(0) = 0.
\end{aligned} \tag{55}$$

Equation (53) reduces to

$$[3(2+c_3)\varphi'''(0) + 4(c+1)R_m(1-\beta_m)]\varphi'''(0) = 0, \tag{56}$$

which gives rise to two subcases:

(B_1) $\varphi'''(0) \neq 0$, $\beta_m > 1$ and

$$\varphi'''(0) = \frac{4R_m(c+1)(\beta_m - 1)}{3(2+c_3)}; \tag{57}$$

(B_2) $\varphi'''(0) = 0$.

We now analyze case (B_1).
If we differentiate twice $(38)_1$, then in $\eta = 0$ we have

$$\varphi^V(0) = (c_2 - c_1)\varphi'''(0). \tag{58}$$

Moreover another differentiation of $(38)_{3,4}$ gives

$$\Phi^{VI}(0) - \Gamma^{VI}(0) = 0. \tag{59}$$

By differentiating $(38)_5$ and (40), we get

$$\Psi^{VI}(0) = 0, \quad \Phi^{VI}(0) - \Gamma^{VI}(0) = 0, \tag{60}$$

and, by differentiating once again, it follows

$$\Phi^{VII}(0) - \Gamma^{VII}(0) = (c-1)\{[15(c_1 - c_2)c_3 + 6c_2]\varphi'''(0) + 4R_m c_2(c+1)(1-\beta_m)\}\varphi'''(0). \tag{61}$$

If we evaluate in $\eta = 0$ the fifth differentiation of $(38)_5$ and of (40), by virtue of (58), (43) then we deduce

$$\Psi^{VII}(0) = -4R_m(c+1)(c_1 - c_2)\varphi'''(0)\Psi'(0),$$

$$\Phi^{VII}(0) - \Gamma^{VII}(0) = 2(c-1)(c_1 - c_2)[-15\varphi'''(0) + 4R_m(\beta_m - 1)(c+1)]\varphi'''(0). \tag{62}$$

Equating (61) and $(62)_2$, we find

$$[15(2 + c_3)(c_1 - c_2) + 6c_2]\varphi'''(0) = 4R_m(c+1)(\beta_m - 1)(2c_1 - c_2). \tag{63}$$

If we take into account (57) and $(22)_{1,2}$, we obtain

$$c_3 = -\frac{24\dfrac{\nu\nu_r}{\lambda a}}{c_2 + 12\dfrac{\nu\nu_r}{\lambda a}}, \tag{64}$$

which gives the absurdum $c_3 < 0$.

To conclude the proof it remains to analyze case (B_2).
The hypotheses $\varphi''(0) = \varphi'''(0) = 0$ furnish

$$\Phi'(0) = 0, \quad \Gamma'(0) = 0. \tag{65}$$

Taking into account (40), system (38) reduces to

$$\varphi''' + (c+1)\varphi\varphi'' + \frac{c\Gamma' - \Phi'}{c-1} - \beta_m(c+1)\Psi\Psi'' = 0,$$

$$\Phi'' + c_3(c+1)\Phi'\varphi - \Phi(cc_3\varphi' + c_2) - c_1\varphi'' = 0,$$

$$\Gamma'' + c_3(c+1)\Gamma'\varphi - \Gamma(c_3\varphi' + c_2) - c_1\varphi'' = 0,$$

$$\Psi'' + R_m(c+1)(\varphi\Psi' - \Psi\varphi') = 0. \tag{66}$$

If we consider the Cauchy problem obtained by adding to (66) the initial conditions

$$\varphi(0) = 0, \ \varphi'(0) = 0, \ \varphi''(0) = 0, \quad \Phi(0) = 0, \ \Phi'(0) = 0,$$

$$\Gamma(0) = 0, \ \Gamma'(0) = 0, \quad \Psi(0) = 0, \ \Psi'(0) = \pm\sqrt{\frac{\beta_m - 1}{\beta_m}}, \tag{67}$$

then its unique solution is given by

$$\varphi(\eta) = 0, \ \Phi(\eta) = 0, \ \Gamma(\eta) = 0, \ \Psi(\eta) = \pm\sqrt{\frac{\beta_m - 1}{\beta_m}}\eta, \quad \forall \eta \in \mathbb{R}^+, \tag{68}$$

which is clearly absurdum because boundary conditions $(39)_{6,9}$ are not satisfied.

References

[1] A.C. Eringen, Theory of micropolar fluids, J. Math. Mech. 16 (1966) 1-18.

[2] K. Das, Slip effects on heat and mass transfer in MHD micropolar fluid flow over an inclined plate with thermal radiation and chemical reaction, Internat. J. Numer. Methods Fluids 70 (2012) 96-113.

[3] T. Hayat, N. Ali, Effects of an endoscope on peristaltic flow of a micropolar fluid, Mathematical and Computer modelling 48 (2008) 721-733.

[4] M. Hussain, M. Ashraf, S. Nadeem, M. Khan, Radiation effects on the thermal boundary layer flow of a micropolar fluid towards a permeable stretching sheet, J. Franklin Inst. 350 (2013) 194-210.

[5] A.C. Eringen, Microcontinuum Field Theories, Vol. $I - II$, Springer-Verlag, 2001.

[6] G. Lukaszewicz, Micropolar Fluids Theory and Applications, Birkäuser, 1999.

[7] J. L. Boldrini, M. Durán, M.A. Rojas-Medar, Existence and uniqueness of strong solution for the incompressible micropolar fluid equations in domains of $\mathbb{R}^3$, Annali Univ. Ferrara 56 (2010) 37-51.

[8] F. Shahzad, M. Sajid, T. Hayat, M. Ayub, Analytic solutions for flow of a micropolar fluid, Acta Mech. 188 (2006) 93-102.

[9] F. Xu Regularity criterion of weak solutions for the 3D Magneto-micropolar fluid equations in Besov spaces, Commun. Nonlinear Sci. Numer. Simulat 17 (2012) 2426-2433.

[10] M. Chen, B. Huang, J. Zhang, Blowup criterion for the three-dimensional equations of compressible viscous micropolar fluids with vacuum, Nonlinear Anal. 79 (2013) 111

[11] A. Borrelli, G. Giantesio, M.C. Patria, Three-dimensional MHD stagnation point-flow of a Newtonian and a micropolar fluid, IJPAM 73 (2011) 165-188.

[12] A. Borrelli, G. Giantesio, M.C. Patria, MHD oblique stagnation-point flow of a micropolar fluid, Applied Math. Model. 36 (2012) 3949-3970.

[13] A. Borrelli, G. Giantesio, M.C. Patria, Numerical simulations of three-dimensional MHD stagnation-point flow of a micropolar fluid, CAMWA 66 (2013) 472-489.

[14] A. Borrelli, G. Giantesio, M.C. Patria, MHD orthogonal stagnation-point flow of a micropolar fluid with the magnetic field parallel to the velocity at infinity, submitted.

[15] A. Borrelli, G. Giantesio, M.C. Patria, Influence of a non-uniform external magnetic field on the oblique stagnation-point flow of a micropolar fluid, submitted.

[16] M. Durán, E.E. Ortega-Torres, M.A. Rojas-Medar, Stationary solutions of magneto-micropolar fluids equations in exterior domains, Proyecciones 22 (2003) 6379.

[17] M. Durán, J. Ferreira, M.A. Rojas-Medar, Reproductive weak solutions of magneto-micropolar fluid equations in exterior domains, Math. Comput. Model. 35 (2002) 779791.

[18] T. Hayat, T. Javed, Z. Abbas, MHD flow of a micropolar fluid near a stagnation-point towards a non-linear streching surface, Nonlinear Analysis: real world application 10 (2009) 1514-1526.

[19] A.M. Abd-Alla, G.A. Yahya, S.R. Mahmoud, H. S. Alosaimi, Effect of the rotation, magnetic field and initial stress on peristaltic motion of micropolar fluid, Meccanica 47 (2012) 1455-1465.

[20] J.M. Dorrepaal, S. Moosavizadeh, Steady incompressible magnethohydrodynamic flow near a point of reattachment, Phys. Fluids 10 (1998) 1512-1518.

[21] T.V.S. Sekhar, R. Sivakumar, H. Kumar, T.V.R. Ravi kumar, Effect of aligned magnetic field on the steady viscous flow past a cricular cylinder, App. Math. Modelling 31 (2007) 130-139.

[22] M.B. Glauert, On magnetohydrodynamic flows with aligned magnetic fields, Fluid Mech. 19 (1963) 49-59.

[23] K. Hiemenz, Die Grenzschicht an einem in den gleichformingen Flussigkeitsstrom eingetauchten graden Kreiszylinder, Dinglers Polytech. J. 326 (1911) 321-324.

[24] F. Homman, Der Einfluss grosser Zahigkeit bei der Stromung um den Zylinder und um die Kugel, Z. Angew. Math. Mech. 16 (1936) 153-164.

[25] C.Y. Wang, Similarity stagnation point solutions of the Navier-Stokes equations-review and extension, Eur. J. Mech. B Fluids 27 (2008) 678683.

[26] M. Ashraf, M.M. Ashraf, MHD stagnation point flow of a micropolar fluid towards a heated surface, Appl. Math. Mech. -Engl. Ed. 32 (2011) 44-54.

[27] J.H. Merkin, Unsteady free convective boundary-layer flow near a stagnation point in a heat-generating porous medium, J. Engrg. Math. 79 (2013) 7389.

[28] R.A. Van Gorder, K. Vajravelu, I. Pop, Hydromagnetic stagnation point flow of a viscous fluid over a stretching or shrinking sheet, Meccanica 47 (2012) 3150.

[29] G.S. Guram, A.C. Smith, Stagnation flows of micropolar fluids with strong and weak interactions, Comp. Maths. with Appls. 6 (1980) 213-233.

[30] G.S. Guram, M. Anwar Kamal, Three-dimensional micropolar flow near saddle and nodal points of attachment, Comp. Maths. Applic. 22 (1991) 1-9.

[31] G. Ahmadi, Self-Similar solution of imcropressible micropolar boundary layer flow over a semi-infinite plate, Int. F. Engng. Sci. 10 (1976) 639-646.

[32] D.A.S. Rees, A.P. Bassom, The Blasius boundary-layer flow of a micropolar fluid, Int. J. Eng. Sci. 34 (1996) 113-124.

[33] Y.Y. Lok, I. Pop, A. J. Chamkha, Non-orthogonal stagnation-point flow of a micropolar fluid, Int. J. Eng. Sci. 45 (2007) 173-174.

[34] R. Nazar, N. Amin, D. Filip, I. Pop Stagnation-point flow of a micropolar fluid towards a stretching sheet, Int. J. of Non-Linear Mech. 39 (2004) 1227-1235.

[35] A. Borrelli, G. Giantesio, M.C. Patria, Effect of a non-uniform external magnetic field on the 3D stagnation-point flow, submitted.
[36] L. F. Shampine, I. Gladwell, S. Thompson, Solving ODEs with MATLAB, Cambridge University Press, 2003.

HIGHLIGHTS (FOR REVIEW)

Ferrara, April, 11th, 2014

Subject: **SUBMISSION OF A REVISED ORIGINAL ARTICLE**

Dear Review,
we send you our revised manuscript: "An exact solution for the 3D MHD stagnation-point flow of a micropolar fluid" for possible publication on Communications in Nonlinear Science and Numerical Simulation.

We have followed your valuable comments on our paper and we have made every change that we have been asked by you.

We recall that in the paper we obtain an exact solution for the steady MHD 3D stagnation-point flow of a homogeneous, incompressible, electrically conducting micropolar fluid. The space is permeated by a not uniform external magnetic field and the total magnetic field in the fluid is parallel to the velocity at infinity. The region where the fluid motion occurs is bordered by the boundary of a solid obstacle which is a rigid uncharged dielectric at rest. In a previous paper we proved that the expression of the electromagnetic field in the solid is formally the same independently of the fluid model over the solid.

By means of similarity transformations, we reduce the MHD PDEs to a nonlinear system of ODEs which depends on three material parameters c_1, c_2, c_3 describing the micropolar nature of the flow and on two parameters R_m (Reynolds number) and β_m (Alfvén number) characterizing the magnetic effects. This system has been numerically integrated and discussed.

The results obtained show that

- The total magnetic field is parallel to the velocity at infinity only if the flow is axisymmetric.
- The thickness of the layer where the viscosity effects appear (boundary layer) depends in a relevant way on R_m and β_m and it is smaller than that in the Newtonian case ([35]).
- The alignment of the magnetic field and of the velocity increases the thickness of the boundary layer in comparison to the case in the absence of the magnetic field and when a uniform magnetic field is applied ([13]).
- The displacement thickness increases as c_2, c_3, β_m increase and c_1, R_m decrease.
- The total magnetic field on the boundary of the solid obstacle increases as β_m, R_m decrease and it is not influenced by the micropolar parameter c_1, c_2, c_3.
- The skin friction increases as c_2, c_3 increase and c_1, β_m, R_m decrease.
- The strength of the skin couple friction increases as c_1 increase and c_2, c_3, β_m, R_m decrease.

- Among the three micropolar parameters c_1, c_2, c_3, the parameter c_1 is the one which influences most the motion.
- The micropolar nature of the fluid reduces all the descriptive quantities of the flow in comparison to the Newtonian case.

Thank you very much for your consideration.
Sincerely yours,

Prof. Alessandra Borrelli, Dott. Giulia Giantesio, Prof. Maria Cristina Patria.